THE ASTROPHYSICAL JOURNAL, 244:230–241, 1981 February 15

TYPE II CEPHEIDS: A COMPARISON OF THEORY WITH OBSERVATIONS

T. RICHARD CARSON, RICHARD STOTHERS, AND SASTRI K. VEMURY
Institute for Space Studies, NASA, Goddard Space Flight Center
Received 1979 December 17; accepted 1980 September 4

ABSTRACT

Theoretical models of normal type II Cepheids in the period range 1–10 days have been constructed with the use of the new Carson opacities. The various features of the computed light and velocity curves are found to agree in detail with those actually observed. For example, the Hertzsprung progression of the light curves shows up distinctly in the approximate period range 1–3 days. Masses of observed type II Cepheids, deduced both from the phase of the Hertzsprung bump in the light curves and from the theoretical pulsation constants, are consistent with each other, and average, formally, $0.59 \pm 0.03\ M_\odot$ for globular cluster members and $0.54 \pm 0.01\ M_\odot$ for the archetypal field variable BL Herculis. These masses also agree closely with masses determined directly from atmospheric analyses and indirectly from stellar-evolution theory. From the location of the observed blue edge of the instability strip in the H-R diagram, the helium abundance in the pulsating layers is inferred to be $0.25 \leq Y \leq 0.50$; and from a comparison of the bump masses and the pulsation-constant masses, it is determined to be $Y = 0.31 \pm 0.08$. This amount of helium is in satisfactory agreement with spectroscopic and evolutionary data for these stars.

If the Cox-Stewart opacities are adopted instead of the Carson opacities, the bump masses turn out to be, at least formally, too small compared to the pulsation-constant masses and to the expected evolutionary masses of the helium cores of these stars, for any realistic helium abundance.

Subject headings: opacities — stars: abundances — stars: Cepheids — stars: pulsation

I. INTRODUCTION

Type II Cepheids are pulsating variable stars belonging to the older population of the Galaxy, with periods ranging upward of 1 day. These low-mass counterparts to the classical Cepheids present an interesting and timely subject for detailed theoretical study, for two reasons. First of all, no nonlinear pulsational models of type II Cepheids have yet been published in detail, with the exception of the 17 day variable W Virginis (Christy 1966*a*; Davis 1972, 1974; Davis and Bunker 1975). Second, there is reason to believe that, from pulsational considerations alone, reliable masses and helium abundances may be derived for these important but rare variable stars. In the present work, we have constructed both linear and nonlinear pulsational models for normal galactic type II Cepheids in the period range 1–10 days, and have compared the results with published observational data. The so-called *anomalous* type II Cepheids are rare or absent in our Galaxy, and will not be considered here; however, their linear pulsational properties have been discussed, for example, by Deupree and Hodson (1977).

The arrangement of our paper is as follows. In § II a quick review of the relevant evolutionary properties of normal type II Cepheids is provided. In the next two sections, we present a detailed survey of the full-amplitude pulsational behavior of model envelopes of these stars, with a discussion of the astronomical implications. In § V we turn to linear pulsation theory in order to delineate the blue edge of the instability strip on the H-R diagram and to discuss period resonances in the models, supplementing the results derived from the nonlinear survey. Our main conclusions are summarized in § VI.

II. EVOLUTIONARY CONSIDERATIONS

The evolutionary status of normal type II Cepheids has been discussed in detail by many authors (see especially Schwarzschild and Härm 1970; Wallerstein 1970; Strom *et al.* 1970; Kraft 1972; Mengel 1973; Sweigart 1973; Zinn 1974; Gingold 1976). It has been found that the isolated position of these stars in the H-R diagram above the RR Lyrae stars and to the left of the red giants effectively constrains their masses and helium abundances to the values $M \approx 0.5–0.6\ M_\odot$ and $Y \approx 0.2–0.3$, if current theories of post-horizontal-branch evolution in globular clusters are correct. Böhm-Vitense *et al.* (1974) have confirmed, on more basic evolutionary grounds, that the masses of these stars must almost certainly lie within the wide bounds $0.4 \leq M/M_\odot \leq 0.8$, the larger value representing the mass of stars now at the main-sequence turnoff in globular clusters and the smaller value representing a lower limit to the possible mass of the helium core in stars evolved to the point of the core helium flash on the red-giant branch. Old Population I Cepheids, however, could conceivably have masses greater than 0.8 $M_\odot$, although they most probably do not.

It is useful (and possible) to have an independent check on the evolutionary masses of type II Cepheids from strictly empirical data. If the definitions of the two atmospheric quantities, surface gravity and radiative flux, are combined into one expression, an "atmospheric" mass can be derived from observations of g, T_e, and L:

$$M = gL/4\pi G\sigma T_e{}^4. \qquad (1)$$

The measured surface gravity, however, is only an "effective" value, g_{eff}, which includes local radiative and inertial forces. But by assuming that radiation pressure can be ignored and that the pulsational radius excursions are small, one can easily prove that the mean value of $\log g_{\text{eff}}$ over a pulsation cycle is equal to $\langle \log g \rangle$. Recently, Smith *et al.* (1978) have published measurements of $\langle \log g_{\text{eff}} \rangle$ and $\langle T_e \rangle$ for the two 1.3 day field variables XX Virginis and BL Herculis. Estimates of $\langle \log L \rangle$ for these stars can be obtained from the mean period-luminosity relation for type II Cepheids, given by Demers and Harris (1974). The masses of XX Vir and BL Her then turn out to be 0.47 ± 0.15 $M_\odot$ and 0.59 ± 0.18 $M_\odot$, respectively, where the errors have been computed from the scatter in the published measurements of $\log g_{\text{eff}}$ and T_e and from the cosmic scatter of $\log L$ around the assumed mean value. These values of the masses are probably more reliable than Wallerstein's (1959*a*) earlier estimates of ~ 1 $M_\odot$ for W Vir and for M5 No. 42. Note also that Norris's (1974) derived atmospheric masses for six nonvariable, bright blue globular-cluster stars average 0.58 ± 0.12 $M_\odot$.

The chemical composition of the pulsating layers of type II Cepheids can also be estimated. Evolutionary theory, as we have indicated, suggests $Y \approx 0.2$–0.3, which is supported by Wallerstein's (1959*b*) coarse analysis of the observed emission lines of hydrogen and helium in W Vir. The nonvariable, bright blue globular-cluster stars also show substantial helium (Norris 1974 and references therein). Although the metal abundance Z is not readily determined from evolutionary theory, which only predicts a qualitative correlation between a high metal abundance and a low stellar mass for type II Cepheids (Cottrell 1979 and references therein), Z is certainly observed to be "very low" among the halo Cepheids and to range up to "nearly normal" for some of the old disk Cepheids (Wallerstein 1959*b*, 1970; Kraft 1972; Smith *et al.* 1978). We may assume that $Z \approx 10^{-4}$ to 10^{-2}.

III. NONLINEAR PULSATIONAL RESULTS

Guided by the foregoing evolutionary considerations, we have selected for our nonlinear survey a set of models with the following parameters: mass, $M/M_\odot = 0.6$; chemical composition, $(X, Y, Z) = (0.745, 0.250, 0.005)$; luminosity, $\log(L/L_\odot) = 2.0$–2.5; and effective temperature, $\log T_e = 3.72$–3.81. The effect of changing Y and Z will be discussed in § IV. One model with $M/M_\odot = 0.8$ has also been calculated.

The computational techniques that we have used to solve the equations of stellar hydrodynamics have been described elsewhere (Vemury and Stothers 1978). Here it suffices to mention our main assumptions about the physics. First, the part of the stellar envelope actually calculated extends from the top of the atmosphere down to a radius fraction of $r/R \approx 0.10$, where the pulsation amplitudes become negligible. Second, the heat flow is calculated by the radiative diffusion approximation at all layers, convection being entirely ignored. Third, the surface boundary conditions are taken from the work of Christy (1967). Fourth, the radiative opacities for $\log T > 3.85$ are derived from the opacity tables described by Carson (1976), with linear interpolation used between tabular grid points; the opacity table for our most frequently used mixture is provided in the Appendix. Cox-Stewart opacities in the form employed by Christy are adopted for $\log T < 3.85$. All the equations are integrated forward in time until the solutions have reached a state in which the physical variables at each mass layer repeat themselves fairly regularly at the same phase from cycle to cycle. Exact repetition is never achieved, partly for numerical reasons but perhaps also from real physical causes, since observed type II Cepheids themselves are not completely regular.

Our main results are summarized in Table 1, which contains, *inter alia*, the following quantities: K.E., peak kinetic energy; Δ, full (not half) amplitude; *Asymmetry*, time spent on the descending branch of the surface velocity curve (or surface luminosity curve) divided by time spent on the ascending branch; ϕ_v, phase, after zero velocity on the ascending branch of the surface velocity curve, of the second (but not necessarily the secondary) bump on this curve, plus unity; and ϕ_l, phase, after mean bolometric magnitude on the ascending branch of the surface luminosity curve, of the second (but not necessarily the secondary) bump on this curve, plus unity. Under the heading *Bump*, the letter A means that the secondary bump appears on the ascending branch, and the letter D means that it appears on the descending branch. If the secondary bump is absent, the letter X is used (XA and XD refer to incipient bumps). The specific definition of this bump will be given below. By the term "surface" we mean the mass layer of the initial equilibrium model where the optical depth is about 0.2.

TABLE 1

FULL-AMPLITUDE PROPERTIES OF THE THEORETICAL MODELS OF TYPE II CEPHEIDS

Parameter	Model 1	2	3	4	5	6	7	8	9
$M/M_\odot$	0.6	0.6	0.6	0.6	0.6	0.6	0.6	0.6	0.8
$\log(L/L_\odot)$	2.00	2.00	2.00	2.25	2.25	2.50	2.50	2.50	2.00
$\log T_e$	3.81	3.78	3.75	3.78	3.75	3.78	3.75	3.72	3.81
$R/R_\odot$	8.13	9.34	10.73	12.49	14.35	16.70	19.21	22.08	8.11
P(days)	1.23	1.63	2.07	2.70	3.52	4.54	5.95	8.44	1.02
K.E. (10^{40} ergs)	1.4	1.6	4.8	4.6	6.7	5.7	7.2	7.6	3.3
$\Delta R/R$	0.16	0.24	0.30	0.36	0.40	0.42	0.34	0.28	0.25
V_{out}(km s^{-1})	31	33	38	47	35	32	23	14	44
V_{in}(km s^{-1})	−42	−44	−44	−59	−36	−32	−33	−37	−36
ΔV(km s^{-1})	74	77	82	106	70	65	56	51	80
L_{max}(10^{35} ergs s^{-1})	5.3	5.5	5.4	9.5	10.0	16.3	16.9	17.7	6.0
L_{min}(10^{35} ergs s^{-1})	2.4	1.7	0.7:	1.9:	3.0:	5.0	4.6	2.9	2.1
ΔM_{bol}	0.9	1.3	2.2	1.8	1.3	1.3	1.4	2.0	1.1
Asymmetry (vel.)	3.6	2.0	2.9	3.2	6.7	3.7	3.6	1.6	4.3
Asymmetry (lum.)	4.1	2.8	1.1	2.1	1.6	1.9	2.2	1.0	4.5
ϕ_v	1.57	1.28	0.94	0.95	0.87	...	...	...	1.67
ϕ_l	1.61	1.25	0.93	0.91	0.89	...	...	...	1.69
Bump	D	D or A	A	A	XA	X	X	X	XD
P_2/P_0	0.54	0.52	0.49	0.48	0.46	0.45	0.42	0.38	0.56

Generally speaking, observed luminosity and velocity curves for these stars show considerable scatter, and it is a common practice among observers to perform an artificial smoothing operation on the curves. By the same token, theoretical luminosity curves and, to a much lesser extent, theoretical velocity curves are also found to be rather noisy near the surface, though mostly for computational reasons. A straightforward smoothing of the calculated curves introduces no appreciable error, provided that the surface pulsations are well behaved. Some of our curves showed so little noise that they required no smoothing; but, for the sake of uniformity, we decided to smooth all the curves by taking a two-point running mean twice in succession. Typically, about 300 models per period were calculated, of which about 60 were used for the plotting. Although the procedure adopted by the observers is different from ours, in that they usually average cycles instead of neighboring points within one cycle, our procedure does provide a means of making an adequate comparison with observations.

Smoothed curves for our models of 0.6 $M_\odot$ are shown in Figures 1 and 2. In all cases, the phases of maximum and minimum velocity (measured positively outward from the center of the star) fall near the respective phases of maximum and minimum luminosity. Although the observed radial-velocity curves of type II Cepheids are of rather rough quality (Joy 1937, 1949; Stibbs 1955; Petit 1960; Abt and Hardie 1960; Lloyd Evans, Wisse, and Wisse 1972; Stobie and Balona 1979; Wallerstein and Brugel 1979), the predic-

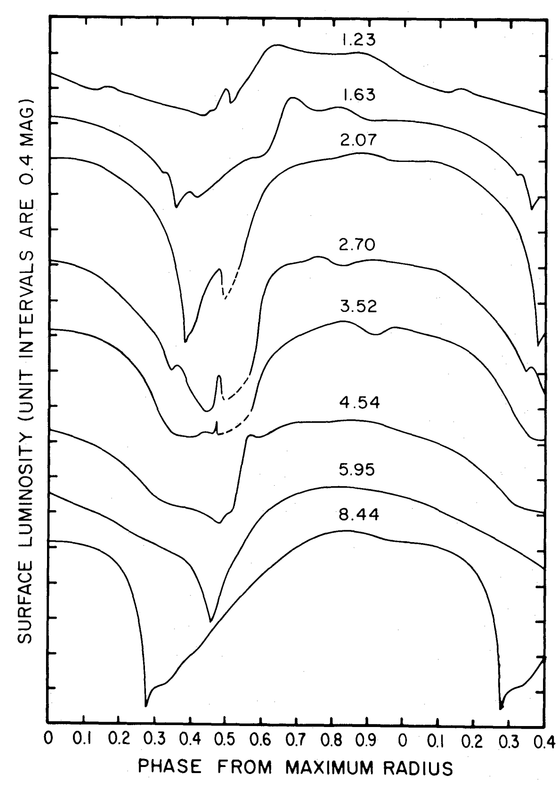

FIG. 1.—Progression of the surface luminosity curves with period for the models of 0.6 $M_\odot$. Dashed segments indicate phases at which the luminosities are unreliable. Periods are given in days.

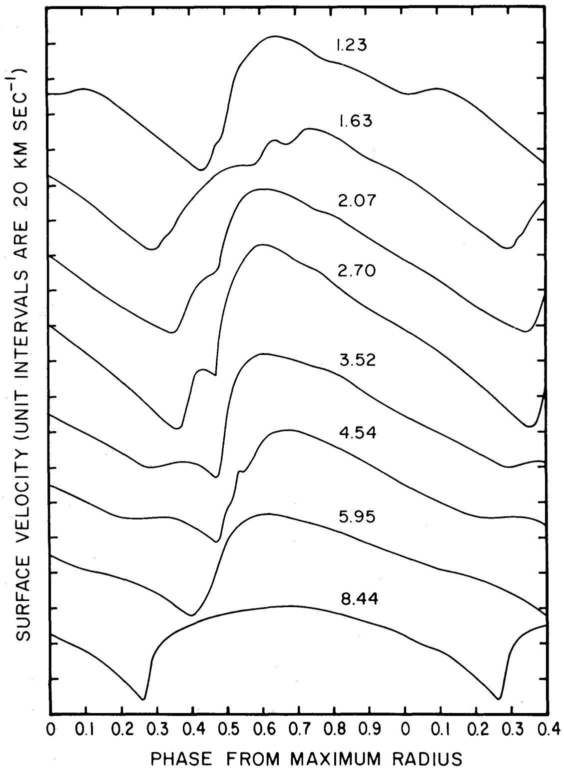

FIG. 2.—Progression of the surface velocity curves with period for the models of 0.6 $M_{\odot}$. Periods are given in days.

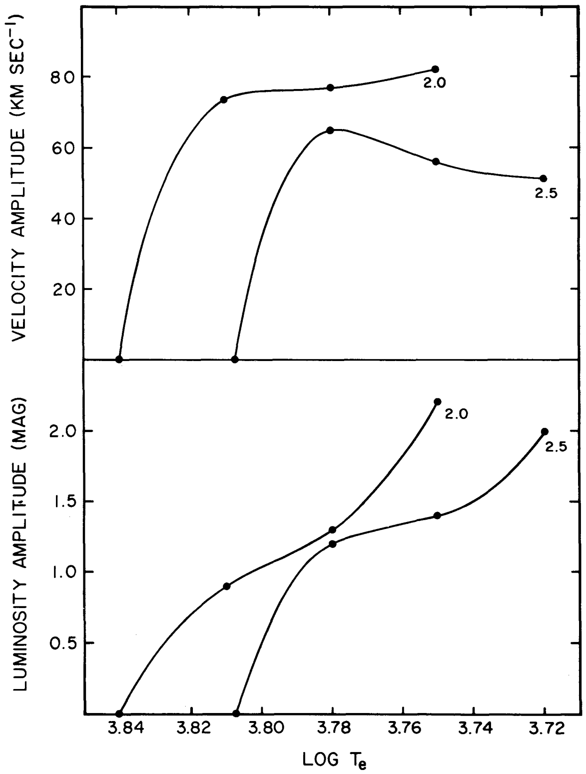

FIG. 3.—Surface velocity and surface luminosity amplitudes versus effective temperature for models of 0.6 $M_{\odot}$. Curves are labeled with $\log(L/L_{\odot})$ values.

ted correlation seems to be adequately confirmed. Unfortunately, unlike the case of the phases, the theoretical amplitudes are much less accurately determined than the observed amplitudes, partly because the theoretical calculation of the atmosphere is so crude but also because the "surface" values in our models refer to a fixed mass layer rather than to the instantaneous photosphere or to the instantaneous line-forming region of the atmosphere. The mean value of the theoretical velocity amplitudes is 70 km s^{-1}. If the observed radial velocities are corrected for geometrical projection and for limb darkening by applying a multiplicative factor of 24/17, the mean value of the observed velocity amplitudes turns out to be 50 km s^{-1}. The modest discrepancy thus appearing between theory and observation is in the same direction and of the same magnitude as the discrepancy that appeared earlier for models of classical Cepheids (Vemury and Stothers 1978). There is a similar discrepancy between the predicted and observed mean luminosity amplitudes, viz., 1.5 mag (theoretical) as against 1.0 mag (observational), the latter value having been reduced by 0.2 mag in order to convert it from a photographic amplitude to a bolometric one. Individual velocity and luminosity amplitudes of the models are shown in Figure 3, including points for the blue edges of the instability strip, where the amplitudes must go to zero. The very large amplitudes predicted at low effective temperatures (cf. also Stellingwerf 1975, Fig. 15) are probably due to our neglect of convection, which, however, would not be expected to significantly alter the periods or shapes of the velocity and luminosity curves (Deupree 1977).

Turning now to the details of these curves, we realize that principal attention must be focused on relations between the *phases* rather than between the *amplitudes* of the various features. It is also apparent that identification of the most important features must rely on the dynamically more fundamental of the two curves, namely, the velocity curve. With this caution, we now draw attention to a secondary bump that develops on the descending branch of both curves at a period of about 1.2 days, at phase 0.5 after velocity maximum. This bump proceeds to drift backward in phase as the period increases, until, at a period of about 1.6 days, it switches from the descending branch to the ascending branch. After the bump reaches the phase of velocity minimum, at a period of about 3.5 days, it effectively disappears. This progression of the bump is the Population II analog of the behavior of a similar feature in models of classical Cepheids with periods longer than ~7 days, the difference of period being due to the difference of stellar mass (§ IV). The interior velocity

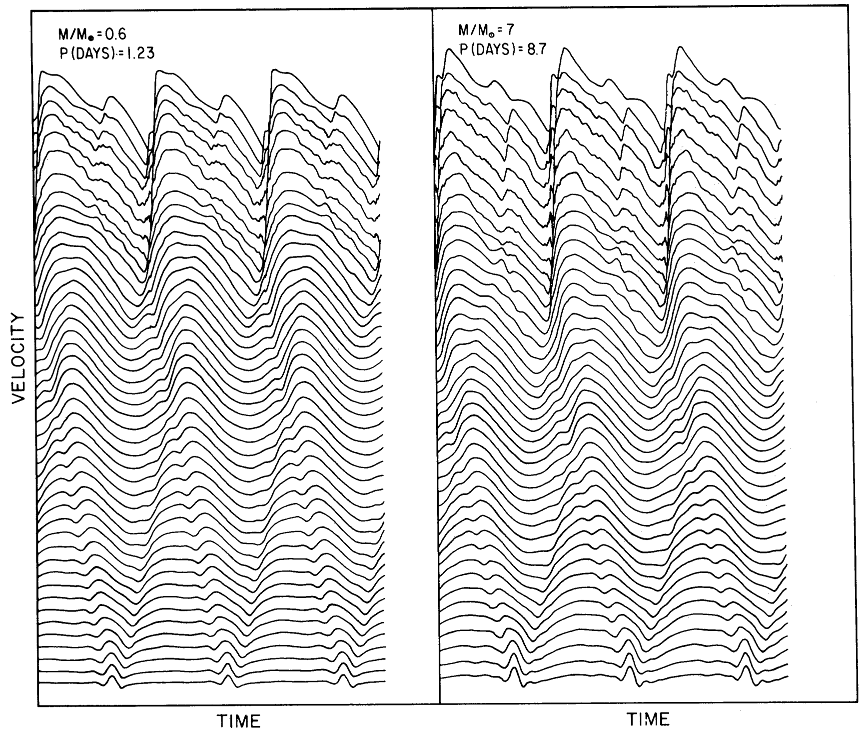

FIG. 4.—Velocity curves for the mass zones in our 1.23 day model for 0.6 $M_\odot$ and for the mass zones in a 8.7 day model for 7 $M_\odot$ (Vemury and Stothers). The vertical scale is different for the various zones.

curves for our 1.23 day model, for example, are shown in Figure 4; they are virtually indistinguishable from those of a 8.7 day classical Cepheid model, which are shown in the same figure for comparison (an earlier, but cruder version of the classical Cepheid plot appeared as Figure 3 in Vemury and Stothers 1978). The immediate cause of the bump is Christy's (1968) "echo phenomenon" (see also Whitney 1956), in which a pressure wave, generated in the helium ionization zone, propagates down to the central core, reflects off it, and arrives at the surface during the next pulsation cycle.

The predicted progression of the bump with period is confirmed by observations. Referred to as the "Hertzsprung progression" in the case of classical Cepheids, it is seen also among type II Cepheids (Stobie 1973; van Genderen 1970, Fig. 1). However, in this paper we shall largely ignore the field Cepheids classified as type II, since their type assignments are often uncertain, except for a few well-observed specimens like BL Her. Thus, in Table 2 we have compiled from various sources the pertinent data on type II Cepheids belonging only to Galactic globular clusters. These data confirm that the progression starts, reaches the switchover point, and ends when the period is, respectively, 1.3, 1.6, and 3–4 days.

Not to be confused with the Hertzsprung bump are two other features which stay relatively fixed in phase and which are seen in the light curves of many Population II variables, ranging from some RR Lyrae stars to probably all W Virginis stars. First is the hump or shoulder that appears around phase 0.2 after light maximum. Second is a shock that appears on the ascending branch of the light curves for periods less than 5 days; when this shock has the same phase as the bump that characterizes the Hertzsprung progression, the effect on the amplitude can be quite remarkable. In contrast, one should compare the smooth, classical-looking light curves for periods of 5–8 days. All of these features are both theoretically predicted and observationally confirmed, although the shoulder on the descending branch is difficult to discern in many of the observed light curves because of its relatively low profile. The absence of observed hydrogen emission in the variables with periods of 5–10 days (Wallerstein 1958; Kraft, Camp, and Hughes 1959) also supports our prediction that no atmospheric shocks occur within this period range.

One type II Cepheid has been observed with such high resolution that it is worth discussing in detail. This is the 1.31 day variable BL Her, studied by Abt and Hardie (1960). Its *U, B, V* light curves and its Hγ and Fe II radial-velocity curves are reproduced in Figure 5, where the radial velocities are shown reversed in sign and multiplied by the conversion factor 24/17. The *V*

TABLE 2

Type II Cepheids with Periods of 1–10 Days in Galactic Globular Clusters

Variable	P(days)	ΔM_{pg}	ϕ_l	Bump	Ref.
ω Cen No. 43.......	1.16	1.1	...	X	1
ω Cen No. 92.......	1.34	0.5	...	X	1
ω Cen No. 60.......	1.35	1.2	1.51	XD	1
M54 No. 1.........	1.35	1.1	[a]	XD?	2
NGC 6752 No. 1....	1.38	1.0	1.50:	XD	3
M15 No. 1.........	1.44	1.3	1.60:	D	1
M13 No. 1.........	1.46	1.4	1.52:	D	1
M56 No. 1.........	1.51	1.0	1.35	D	4
M22 No. 11........	1.69	0.7	[a]	D or A	5
M14 No. 76........	1.89	0.9	0.89	A	6
M13 No. 6.........	2.11	0.9	0.88	A	1
ω Cen No. 61.......	2.27	0.8	0.89	A	1
M19 No. 4.........	2.43	1.7	0.90:	A	7
M14 No. 2.........	2.79	1.2	0.90	A	8
ω Cen No. 48.......	4.47	0.9	...	X	1
M13 No. 2.........	5.11	1.2	...	X	1
M10 No. 3.........	7.91	0.8	...	X	1

[a] Published light curve is inadequate to locate the secondary bump.

References—(1) Arp 1955; (2) Rosino and Nobili 1959; (3) Lee 1974; (4) Rosino 1944; (5) Wehlau and Sawyer Hogg 1978; (6) Sawyer Hogg and Wehlau 1968; (7) Coutts Clement and Sawyer Hogg 1978; (8) Sawyer Hogg and Wehlau 1966.

light curve should correspond approximately to the star's bolometric light curve, except during the brief interlude of the premaximum shock, when hydrogen emission is prominently visible at shorter wavelengths.

For comparison, we show in Figure 5 the luminosity and velocity curves for our theoretical model with 1.23 day period. It is immediately evident that the amplitudes and asymmetries of these curves agree remarkably well with those observed for BL Her, especially when one realizes that the theoretical velocity curve refers, roughly, to optical depth ~0.2 whereas the Hγ and Fe II curves refer to optical depths that are, respectively, smaller and larger than this. Moreover, with respect to the phase of velocity maximum, the theoretical phases of light maximum, postmaximum shoulder, Hertzsprung bump, and premaximum shock are in essentially exact agreement with observations. As expected, the minor features show up more clearly in the light curves than in the velocity curves; in fact, in the case of the observed velocity curves, only the Hertzsprung bump can be recognized (note that we have used for these curves the observed velocity *points* given by Abt and Hardie, whose published velocity *curves* do not include the bump or inflection near phase 0.5). The even smaller details along the rising branch of the theoretical light and velocity curves can be compared with Preston and Kilston's (1967) observations at these phases. They found that the premaximum shock (which appears as a stillstand in visual wavelengths) occurs shortly before mean light and at about the phase when the velocity curve changes its slope, so that mean

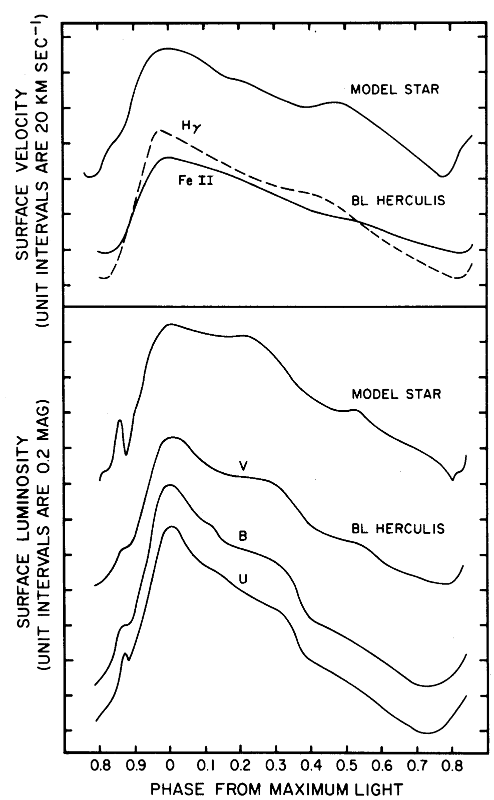

Fig. 5.—Surface velocity and surface luminosity curves for BL Herculis (Abt and Hardie) and for our model with 1.23 day period. The radial velocities of BL Herculis have been transformed to the astrocentric coordinate system.

light is delayed by 0.05 of a period after mean velocity. A check of the theoretical model reveals precisely the same phase relations.

BL Herculis also provides us with an important check on the theoretical values of the phase quantities ϕ_v and ϕ_l, which we defined earlier. The observed values are $\phi_v = 1.55 \pm 0.05$ and $\phi_l = 1.59 \pm 0.01$, which are to be compared with theoretical values of $\phi_v = 1.57$ and $\phi_l = 1.61$ taken from the model. Observation and theory thus concur that $\phi_v \approx \phi_l$. The small discrepancy of 6% between the observed and computed periods can easily be removed by a minor adjustment of the stellar mass and radius (see next section). The only other discrepancy between our model and BL Herculis is the differing amplitude of the postmaximum shoulder on the light curve; the cause of the difference is unknown.

It may be noted here that XX Vir, which has very nearly the same period as BL Her, shows a much smoother light curve (with only a hint of the Hertzsprung bump at $\phi_l \approx 1.56$) even though its light and velocity amplitudes are larger (Wallerstein and Brugel 1979). On theoretical grounds, this difference in behavior can most likely be attributed to small differences of mass, luminosity, and effective temperature, in analogy with what we previously obtained for models of classical Cepheids (Vemury and Stothers 1978). Those models showed that there exists a small period range, close to the period when the Hertzsprung bump first appears, in which the bump may or may not be prominent, regardless of the star's total pulsation amplitude, with the exception that, in general, a star with a very low amplitude cannot show the bump since the bump is a threshold phenomenon. For classical Cepheids, the period range in question is 6–8 days; by a scaling argument, we anticipate that the period range will be 1.1–1.4 days for type II Cepheids. XX Virginis falls in this period range. We may add here that UY Eri and ω Cen No. 92 also do not show the bump; the reason is probably that the amplitudes of these two stars are too low.

New data have very recently become available for the 1.58 day variable SW Tau, which shows, approximately, $\phi_v \approx 1.46$ and $\phi_l \approx 1.51$ (Stobie and Balona 1979). Again, we establish that $\phi_v \approx \phi_l$.

IV. PULSATIONAL MASSES

The "pulsation constant" for any periodically pulsating star is defined as

$$Q = P(M/M_\odot)^{1/2}(R/R_\odot)^{-3/2}. \tag{2}$$

It is well known that Q is approximately proportional to $(R/M)^{1/4}$ for a wide range of stellar models pulsating in the fundamental radial mode (Christy 1966*b*). Our present results, including those derived for a variety of assumed masses and chemical compositions (§ V), may be expressed as

$$P \approx 0.022(R/R_\odot)^{7/4}(M/M_\odot)^{-3/4} \text{ days}, \tag{3}$$

where the coefficient has a scatter of ± 0.001.

Notice that equation (3) is simply another form of the familiar period-luminosity relation, modified by additional terms taking into account stellar mass and effective temperature, the radius being eliminated by the use of Stefan's law, $L = 4\pi R^2 \sigma T_e{}^4$. The general form of the period-luminosity relation is $P \propto L^{0.87} T_e{}^{-3.5} M^{-0.75}$. It agrees very well with the observational data of Böhm-Vitense *et al.* (1974), provided that M is constant.

Stellar masses can be derived from equation (3) if the pulsation periods and mean stellar radii are known. Among the galactic type II Cepheids with periods of 1–10 days, Böhm-Vitense *et al.* (1974) have determined accurate photometric radii for UY Eri, M13 No. 6, and M10 No. 3, to which we may add the reliable Wesselink radius for BL Her given by Abt and Hardie (1960). These four stars yield an average pulsational mass of $\langle M/M_\odot \rangle = 0.56 \pm 0.05$. We have decided not to use the Wesselink radii published for κ Pav, V553 Cen, and SW Tau (Rodgers 1957; Balona 1977; Stobie and Balona 1979), because the validity of the Wesselink method for these three stars has not yet been established.

An independent way of estimating the radius of a type II Cepheid is applicable to those stars that show the Hertzsprung bump. Plausible physical arguments have suggested that the product $P\phi_v$ ought to be nearly proportional to R, if ϕ_v is defined as above (e.g., Christy 1968; Fricke, Stobie, and Strittmatter 1972). From our models we find that

$$P\phi_v \approx 0.21(R/R_\odot) \text{ days}, \tag{4}$$

with a scatter of ± 0.03 in the coefficient. If we now introduce the (P, M, R) relation into equation (4), the mass, too, can be estimated from P and ϕ_v:

$$M/M_\odot \approx 0.24 P\phi_v^{7/3}, \tag{5}$$

which agrees well with the result derived for classical Cepheids (Vemury and Stothers 1978). Alternatively, we are permitted to substitute ϕ_l for ϕ_v in both equations (4) and (5), because, for type II Cepheids,

$$\phi_v - \phi_l = 0.00 \pm 0.04. \tag{6}$$

Since equation (5) has only approximate statistical validity (even in general form), it cannot be expected to furnish a very accurate mass for any individual type II Cepheid—the estimated error of the mass arising from scatter among the theoretical models alone is about 35%.

For the 10 globular-cluster Cepheids listed in Table 2 whose phases ϕ_l can be estimated at least roughly from the published light curves, we have determined, in this way, an average bump mass of $\langle M/M_\odot \rangle = 0.65 \pm 0.08$. Improved masses can be derived by direct interpolation in Table 1; the average bump mass then turns out to be $\langle M/M_\odot \rangle = 0.60 \pm 0.03$.

BL Herculis is the one type II Cepheid which can be analyzed very accurately as an individual star. By interpolating with P and ϕ_l among the models in Table 1, the mass of BL Her comes out to be 0.54 ± 0.01 $M_\odot$. Its radius, in similar fashion, is found to be 8.1 ± 0.1 $R_\odot$, which agrees excellently with an empirical radius of 8.3 ± 0.6 $R_\odot$ obtained by the use of a corrected form of Wesselink's method (Abt and Hardie 1960). If we now interpolate with the observed P and R in Table 1, we obtain another estimate of the mass, 0.57 ± 0.13 $M_\odot$.

It is also possible to estimate the helium abundance in the pulsating layers of type II Cepheids, by using the circumstance that the (P, M, R) relation is independent of Y whereas the (P, M, ϕ_v) relation is not. For classical Cepheids, the mass derived from the (P, M, ϕ_v) relation is known to be approximately proportional to $Y^{-0.3}$ (Fricke, Stobie, and Strittmatter 1971; Vemury and Stothers 1978). This dependence on Y, because it is principally an effect of mean molecular weight, may be assumed to apply equally well to type II Cepheids. By forcing the mass derived from the (P, M, R) relation to be equal to the mass derived from the (P, M, ϕ_v) relation, Y can be estimated. Application of this method to BL Her yields $Y = 0.21 \pm 0.19$; for our whole sample of type II Cepheids, $Y = 0.31 \pm 0.08$. The rather large uncertainty in the derived helium abundance arises almost entirely from the uncertainty of the observed radii.

The metal abundance Z turns out to be an unimportant factor, as we have established by a recalculation of our 1.23 day model with $Z = 0$. The new model has $\phi_v = 1.55$ and $\phi_l = 1.58$, which, together with other computed properties, agree well with the model results for $Z = 0.005$.

It remains to compare our results based on the Carson opacities with a parallel set of results based on the Cox-Stewart opacities. Böhm-Vitense *et al.* (1974) have published a (P, M, R) relation derived by the use of the Cox-Stewart opacities. This relation, applied to the same four stars that we used above, yields $\langle M/M_\odot \rangle = 0.52 \pm 0.05$ (essentially as those authors also found). Evidently, the choice of opacities makes little difference for the masses derived in this way.

The situation is very different in the case of the (P, M, ϕ_v) relation, which, for Cox-Stewart opacities, has been obtained by Stobie (1973) and also, implicitly, by Christy (1970, 1975), although for these opacities the relation was based mostly on classical Cepheid models. Stobie's explicit relation, when applied to our sample of 10 globular-cluster Cepheids, yields a very low average mass, $\langle M/M_\odot \rangle = 0.40 \pm 0.06$. Although Stobie himself derived a larger value of ~ 0.55 $M_\odot$ for his sample of type II Cepheids, his result is marred by two procedural errors. First, he assumed a tentative (ϕ_l, ϕ_v) relation based on observations of *classical* Cepheids, namely, $\phi_v - \phi_l \approx 0.2$ (which, incidentally, needs to be checked for classical Cepheids themselves). Second, he seems to have misidentified the Hertzsprung bump, or else measured the phase ϕ_l incompatibly with its definition, for most of the type II Cepheids in his list. His sample of stars is actually found to yield an average pulsational mass, corrected, of ~ 0.32 $M_\odot$. Since the expected mass of the helium core in these stars is ~ 0.45 $M_\odot$, and since a total mass smaller than this is astrophysically unrealistic, we conclude that the use of the Cox-Stewart opacities seems to lead to an incorrect (P, M, ϕ_v) relation. This conclusion has already been reached in the case of the classical Cepheids (Vemury and Stothers 1978).

In order to be absolutely certain of this conclusion for type II Cepheids, we have computed another nonlinear model for BL Her, having the same mass, composition, radius, period, and amplitude as our 1.23 day model, but based on Cox-Stewart opacities in the form used by Christy. This model's luminosity and effective temperature are $\log(L/L_\odot) = 1.88$ and $\log T_e = 3.78$. The resulting luminosity and velocity curves turn out to be different in four important respects from what we obtained with the use of the Carson opacities: first, the luminosity maximum is split into two subpeaks; second, the postmaximum shoulder is significantly broadened; third, the premaximum shock is virtually absent; and fourth, the phase of the Hertzsprung bump is delayed (in qualitative agreement with Stobie's and Christy's results), now occurring at $\phi_v = 1.75$ and $\phi_l = 1.73$. Thus, the results based on the Cox-Stewart opacities do not seem to agree with Abt and Hardie's observational data for BL Her.

V. LINEAR PULSATIONAL RESULTS

To supplement the nonlinear results of §§ III and IV, we have resorted to linear nonadiabatic theory (which is a much faster method) for the calculation of (a) the blue edges of the instability strip in the H-R diagram and (b) the period ratios between the fundamental mode, first overtone, and second overtone. Physical assumptions in the models are the same as before, except for the surface boundary conditions, which are now applied at the photosphere (Baker-Kippenhahn boundary conditions). We have already shown that this slight incompatibility in the methods causes very little difference in the derived results for linear and nonlinear models of classical Cepheids (Vemury and Stothers 1978); therefore it is reasonable to suppose that the same is true for models of type II Cepheids.

TABLE 3

THEORETICAL BLUE EDGES OF THE TYPE II CEPHEID INSTABILITY STRIP[a]

$M/M_{\odot}$	Y	Z	$(\log T_e)_0$ for $\log(L/L_{\odot})=2.0$	$(\log T_e)_0$ for $\log(L/L_{\odot})=2.5$	$(\log T_e)_0$ for $\log(L/L_{\odot})=3.0$
0.4.......	0.25	0.0	3.809	3.735	...
0.6.......	0.25	0.0	3.826	3.767	3.68:
	0.25	0.005	3.840	3.807	3.763
	0.25	0.010	3.842	3.820	3.808
	0.25	0.020	3.848	3.836	3.838
	0.50	0.0	3.861	3.829	3.773
	0.75	0.0	3.872	3.851	3.814
0.8.......	0.25	0.0	3.834	3.784	3.724
1.0.......	0.25	0.0	3.837	3.796	3.740

[a] Based on linear nonadiabatic theory.

a) *Blue Edges*

A large number of theoretical blue edges with different combinations of the assignable parameters has been computed. Some of our results for the fundamental mode are shown in Table 3 and in Figure 6. In the case of our standard parameters, viz., $M/M_{\odot}=0.6$, $Y=0.25$, and $Z=0.005$, the first and second overtones are found to be stable at all effective temperatures tested. These modes do become unstable (in the linear approximation) for higher values of M, Y, and Z, but it is also known that the stability of overtones, in general, is extremely sensitive to small changes in surface boundary conditions, method of interpolating the opacity tables, etc. (Iben 1971; Tuggle and Iben 1972). Therefore, we do not consider the blue edges for the overtones further.

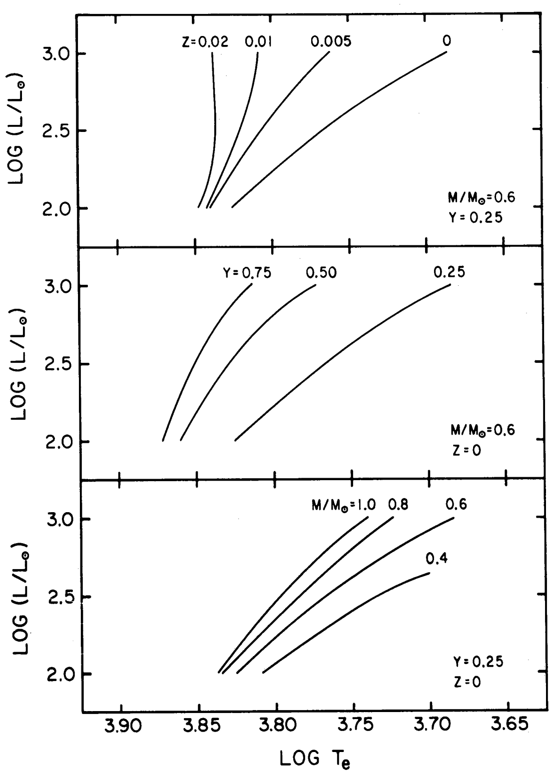

FIG. 6.—Theoretical blue edges of the instability strip (for the fundamental mode) in the H-R diagram.

The sensitivity of the fundamental blue edges to the parameters M and Y is not surprising, because it has already been indicated by calculations based on Cox-Stewart opacities (Iben and Huchra 1971; Iben 1971; Tuggle and Iben 1972; Cox and King 1972; Cox, King, and Tabor 1973; Bednarek 1975; Deupree and Hodson 1977). However, the dependence on Z is a unique feature of the new opacities, as discussed by Carson and Stothers (1976). Not a great deal of reliability can be placed on the exact locations of the derived blue edges, for a number of reasons. For one thing, if the Baker-Kippenhahn boundary conditions were replaced by the Castor-Iben ones, the blue edges would probably be shifted to higher values of $\log T_e$ by about 0.03 (Iben 1971). For another thing, if convection were introduced, or if a finer grid in the opacity tables or else a more refined method of interpolating the opacity tables were used, the blue edges would again be shifted, the amount of the shift depending to a large extent on the luminosity adopted. For one composition mixture, $(X, Y, Z)=(0.730, 0.250, 0.020)$, an opacity table with twice the resolution of our standard table is available; the resulting shift in $\log T_e$, however, is found to be negligible at $\log(L/L_{\odot})=2.0$ and only -0.003 at $\log(L/L_{\odot})=2.5$, for a stellar mass of 0.6 $M_{\odot}$. Similarly, the use of *quadratic* interpolation in our *standard* opacity table leads to respective shifts in $\log T_e$ of -0.004 and $+0.001$. These results suggest that our adopted procedures with respect to the opacity tables are adequate for the linear models and probably also for the nonlinear models, since in the latter case the thermodynamic derivatives of opacity do not need to be calculated and the explicit time integration smooths out the effects of irregularities in the opacity values.

To compound the difficulties incurred by the poorly known surface boundary conditions, however, the location of the observed blue edge itself is uncertain. Demers and Harris (1974) have tentatively placed it near $\log T_e = 3.86$ at $\log(L/L_\odot) = 2.0$ and near $\log T_e = 3.77$ at $\log(L/L_\odot) = 3.0$. The possible error of these $\log T_e$ values must be at least ± 0.04, if a correct judgment can be formed from consideration of the empirical blue edge derived by Böhm-Vitense *et al.* (1974).

Taking proper account of both observational and theoretical uncertainties, we find that acceptable agreement between the predicted and observed blue edges can be obtained if $0.25 \leq Y \leq 0.50$ and $0 \leq Z \leq 0.01$, provided only that $M/M_\odot \approx 0.6$. Approximately the same result is found by using stellar models based on the Cox-Stewart opacities. Although blue edges for the latter opacities are slightly cooler than the ones we have derived (after adjusting them all to the same surface boundary conditions), this difference is not very significant compared to the differences arising from all the other uncertainties.

b) *The Resonance* $P_2/P_0 = 0.5$

Simon and Schmidt (1976) have pointed out that an apparent correlation exists between the presence of the Hertzsprung bump in the light curves of classical Cepheids and the occurrence of a period resonance $P_2/P_0 = 0.5$ in linear models of these stars. Various scaling arguments based on our new nonlinear results suggest that a formally identical resonance should show up in models of type II Cepheids along *their* Hertzsprung progression. To see if this is indeed the case, we have computed second-overtone periods, P_2, for the models in Table 1; our results are given at the bottom of the table. It is evident that the models with the Hertzsprung bump on the descending branch ($P_0 = 1.0$–1.6 days) have $P_2/P_0 = 0.51$–0.56 and that the models with the Hertzsprung bump on the ascending branch ($P_0 = 1.6$–3.5 days) have $P_2/P_0 = 0.46$–0.51. The resonance band thus derived is identical to the one which we obtained previously for classical Cepheid models.

One difference between the two types of Cepheid models is important, however: for type II Cepheids, P_2/P_0 decreases much more rapidly with increasing P_0. Extension of the linear calculations to models of type II Cepheids with very long periods indicates that, when $P_0 \approx 14$ days, the models are characterized by the resonance $P_2/P_0 = 0.333$. Even more interesting is the fact that a resonance between the first overtone and the fundamental mode, $P_1/P_0 = 0.5$, occurs when $P_0 \approx 17$ days. If the full width of the resonance band in this case is assumed to be the same as for the P_2/P_0 band at shorter fundamental periods, then the full P_1/P_0 band will cover the period range $P_0 = 10$–25 days. Now, according to Simon and Schmidt's hypothesis, a resonance between the two lowest pulsation modes would be expected to modulate the surface amplitudes in an even more significant way than would any higher resonance. Yet no analog of the Hertzsprung progression is observed among type II Cepheids of this period range (see, e.g., Arp 1955). This fact reinforces our previously expressed (Vemury and Stothers 1978) reservation about the physical significance of the period ratios.

VI. CONCLUSION

From the present detailed study of normal type II Cepheids has emerged some new theoretical understanding of these stars and, we hope, some practical information. Basic astrophysical data, like masses and helium abundances, have been successfully derived. Our results for the masses of type II Cepheids are summarized in Table 4. Since the methods used in deriving these masses are independent of each other, the close agreement of the various results is encouraging. In fact, the slightly smaller mass found for BL Her compared with globular cluster stars may be significant, since BL Her is relatively metal-rich.

The helium abundance is more difficult to determine than the masses, but may be estimated by using the blue edge of the instability strip in the H-R diagram. This approach leads to $0.25 \leq Y \leq 0.50$, for $0 \leq Z \leq 0.01$, Forcing the masses inferred from the theoretical pulsation constants to agree with those inferred from the observed phases of the Hertzsprung bump leads to $Y = 0.31 \pm 0.08$ (for globular-cluster Cepheids). Evolutionary theory suggests $0.2 \leq Y \leq 0.3$, and rough spectroscopic data point to an equally substantial helium abundance.

It should be stressed that none of these results is particularly sensitive to the opacities adopted in the theoretical models, with the exception of the results based on the Hertzsprung bump. We point out that the present models have been constructed on the basis of a new set of opacities, which, for the elements most important to Cepheid pulsation, viz., hydrogen and helium, have been calculated with probably the same

TABLE 4

MASSES OF TYPE II CEPHEIDS IN THE PERIOD RANGE 1–10 DAYS[a]

Method	Average Globular Cluster Cepheid	BL Herculis
Q value	0.56 ± 0.05	0.57 ± 0.13
Hertzsprung bump	0.60 ± 0.03	0.54 ± 0.01
Atmospheric analysis	0.58 ± 0.12[b]	0.59 ± 0.18
Evolutionary tracks	0.55 ± 0.05	...
Mean	0.58 ± 0.02	0.54 ± 0.01

[a] Masses in solar units.

[b] Derived for nonvariable, bright blue stars in globular clusters (Norris 1974).

degree of accuracy as have the Cox-Stewart opacities. Had the Cox-Stewart opacities been adopted, however, the stellar masses inferred from the Hertzsprung bump would have turned out to be less than the stellar core masses, unless the envelope helium abundance were as low as $Y \approx 0.15$, which would contradict the other evidence on this point. Although the formal errors of many of our results in this paper seem rather small, it must be remembered that they have been computed, for *each* set of opacities, as if both the opacities and the stellar models were error-free. The true (unknown) errors will be larger, since neither set of opacities is definitive and Y is not known exactly.

Lastly, we wish to emphasize the agreement in detail between our theoretically computed light curves and those actually observed. To the best of our knowledge, the precision that we have attained in modeling BL Her has not been achieved before in the case of any variable star. Extension of the present calculations to other kinds of variable stars in the Cepheid instability strip would therefore be a useful immediate step.

We thank Helen Sawyer Hogg for her generosity in helping us to compile Table 2, and Olenka Hubickyj for deriving two of the nonlinear models. T. R. C. wishes to acknowledge the award of a Senior Visiting Fellowship by the Science Research Council of the United Kingdom, and also the use of the facilities of the University of Cambridge Computer Laboratory.

REFERENCES

Abt, H. A., and Hardie, R. H. 1960, *Ap. J.* **131**, 155.
Arp, H. C. 1955, *Ap. J.*, **60**, 1.
Balona, L. A. 1977, *M.N.R.A.S.*, **178**, 231.
Bednarek, T. A. 1975, in *Cepheid Modeling*, ed. D. Fischel and W. M. Sparks (Washington: NASA), p. 115.
Böhm-Vitense, E., Szkody, P., Wallerstein, G., and Iben, I., Jr. 1974, *Ap. J.*, **194**, 125.
Carson, T. R. 1976, *Ann. Rev. Astr. Ap.*, **14**, 95.
Carson, T. R., and Stothers, R. 1976, *Ap. J.*, **204**, 461.
Christy, R. F. 1966*a*, *Ap. J.*, **145**, 337.
______. 1966*b*, *Ann. Rev. Astr. Ap.*, **4**, 353.
______. 1967, in *Methods in Computational Physics*, ed. B. Alder (New York: Academic Press), Vol. **7**, p. 191.
______. 1968, *Quart. J.R.A.S.*, **9**, 13.
______. 1970, *J.R.A.S. Canada*, **64**, 8.
______. 1975, in *Cepheid Modeling*, ed. D. Fischel and W. M. Sparks (Washington: NASA), p. 85.
Cottrell, P. L. 1979, *M.N.R.A.S.*, **189**, 13.
Coutts Clement, C., and Sawyer Hogg, H. 1978, *A.J.*, **83**, 167.
Cox, A. N., King, D. S., and Tabor, J. E. 1973, *Ap. J.*, **184**, 201.
Cox, J. P., and King, D. S. 1972, in *The Evolution of Population II Stars*, ed. A. G. D. Philip (Albany, NY: Dudley Observatory), p. 103.
Davis, C. G., Jr. 1972, *Ap. J.*, **172**, 419.
______. 1974, *Ap. J.*, **187**, 175.
Davis, C. G., Jr., and Bunker, S. S. 1975, in *Cepheid Modeling*, ed. D. Fischel and W. M. Sparks (Washington: NASA), p. 71.
Demers, S., and Harris, W. E. 1974, *A.J.*, **79**, 627.
Deupree, R. G. 1977, *Ap. J.*, **211**, 509.
Deupree, R. G., and Hodson, S. W. 1977, *Ap. J.*, **218**, 654.
Fricke, K., Stobie, R. S., and Strittmatter, P. A. 1971, *M.N.R.A.S.*, **154**, 23.
______. 1972, *Ap. J.*, **171**, 593.
Gingold, R. A. 1976, *Ap. J.*, **204**, 116.
Iben, I., Jr. 1971, *Pub. A.S.P.*, **83**, 697.
Iben, I., Jr., and Huchra, J. 1971, *Astr. Ap.*, **14**, 293.
Joy, A. H. 1937, *Ap. J.*, **86**, 363.
______. 1949, *Ap. J.*, **110**, 105.
Kraft, R. P. 1972, in *The Evolution of Population II Stars*, ed. A. G. D. Philip (Albany, NY: Dudley Observatory), p. 69.
Kraft, R. P., Camp, D. C., and Hughes, W. T. 1959, *Ap. J.*, **130**, 90.
Lee, S. W. 1974, *Observatory*, **94**, 74.
Lloyd Evans, T., Wisse, P. N. J., and Wisse, M. 1972, *M.N.R.A.S.*, **159**, 67.
Mengel, J. G. 1973, in *Variable Stars in Globular Clusters and Related Systems*, ed. J. D. Fernie (Dordrecht: Reidel), p. 214.
Norris, J. 1974, *Ap. J.*, **194**, 109.
Petit, M. 1960, *Ann. d'Ap.*, **23**, 681.
Preston, G. W., and Kilston, S. D. 1967, *Ap. J.*, **148**, 787.
Rodgers, A. W. 1957, *M.N.R.A.S.*, **117**, 85.
Rosino, L. 1944, *Pub. Oss. Bologna*, **4**, No. 7.
Rosino, L., and Nobili, F. 1959, *Contr. Oss. Padova Asiago*, No. 97.
Sawyer Hogg, H., and Wehlau, A. 1966, *Pub. David Dunlap Obs.*, Vol. **2**, No. 17.
______. 1968, *Pub. David Dunlap Obs.*, Vol. **2**, No. 19.
Schwarzschild, M., and Härm, R. 1970, *Ap. J.*, **160**, 341.
Simon, N. R., and Schmidt, E. G. 1976, *Ap. J.*, **205**, 162.
Smith, H. A., Jacques, J., Lugger, P. M., Deming, D., and Butler, D. 1978, *Pub. A.S.P.*, **90**, 422.
Stellingwerf, R. F. 1975, *Ap. J.*, **195**, 441.
Stibbs, D. W. N. 1955, *M.N.R.A.S.*, **115**, 363.
Stobie, R. S. 1973, *Observatory*, **93**, 111.
Stobie, R. S., and Balona, L. A. 1979, *M.N.R.A.S.*, **189**, 641.
Strom, S. E., Strom, K. M., Rood, R. T., and Iben, I., Jr. 1970, *Astr. Ap.*, **8**, 243.
Sweigart, A. V. 1973, *Astr. Ap.*, **24**, 459.
Tuggle, R. S., and Iben, I., Jr. 1972, *Ap. J.*, **178**, 455.
van Genderen, A. M. 1970, *Astr. Ap.*, **7**, 244.
Vemury, S. K., and Stothers, R. 1978, *Ap. J.*, **225**, 939.
Wallerstein, G. 1958, *Ap. J.*, **127**, 583.
______. 1959*a*, *Ap. J.*, **129**, 356.
______. 1959*b*, *Ap. J.*, **130**, 560.
______. 1970, *Ap. J.*, **160**, 345.
Wallerstein, G., and Brugel, G. W. 1979, *A.J.*, **84**, 1840.
Wehlau, A., and Sawyer Hogg, H. 1978, *A.J.*, **83**, 946.
Whitney, C. 1956, *A.J.*, **61**, 192.
Zinn, R. J. 1974, *Ap. J.*, **193**, 593.

T. RICHARD CARSON: University Observatory, Buchanan Gardens, St. Andrews, Fife, Scotland

RICHARD STOTHERS and SASTRI K. VEMURY: Institute for Space Studies, NASA Goddard Space Flight Center, 2880 Broadway, New York, NY 10025

APPENDIX

TABLE 5

OPACITIES FOR COMPOSITION $X=0.745$, $Y=0.250$, $Z=0.005$

LOG RHO / LOG T	I	LOG OPACITY (CM2/G) I	I+1	I+2	I+3	I+4	I+5	I+6	I+7	I+8
3.7	-11	-1.9779	-1.9705	-1.9013	-1.7007	-1.2560	-0.5382	0.2443	2.3289	1.6082
3.8	-11	-1.3903	-1.4450	-1.2386	-0.8230	-0.3139	0.2392	0.8537	4.1703	2.0458
3.9	-11	-0.2225	-0.1245	0.0269	0.2715	0.6000	1.1787	1.4831	2.0504	2.7664
4.0	-11	-0.1104	0.5225	1.1324	1.4191	1.6507	1.9237	2.2925	2.7358	3.3808
4.1	-10	0.2267	1.1307	1.9500	2.4716	2.7803	3.0655	3.3787	3.9152	4.6178
4.2	-10	-0.0546	0.6911	1.6666	2.6372	3.3011	3.7073	3.9833	4.4218	3.4081
4.3	-10	-0.2298	0.3405	1.2726	2.3148	3.3148	4.1228	4.4683	4.8190	4.7931
4.4	-10	-0.2831	0.1263	0.9868	2.0444	3.1526	4.2636	4.9070	5.2222	5.0725
4.5	-10	-0.2294	0.0762	0.8292	1.8628	2.9966	4.1983	5.0334	5.3458	3.2087
4.6	-9	0.1447	0.8299	1.7775	2.8392	3.9969	4.8806	5.4537	4.0504	5.6462
4.7	-9	-0.1331	0.7417	1.7168	2.6845	3.6669	4.5248	5.2311	4.6848	5.4636
4.8	-9	-0.2661	0.4521	1.1932	2.3241	3.2684	4.1628	4.8975	4.8619	5.2617
4.9	-9	-0.2356	0.1163	0.7641	1.8489	2.8130	3.8401	4.6103	4.8340	5.0676
5.0	-9	-0.3476	-0.0991	0.5454	1.4797	2.4406	3.5172	4.3616	4.6592	4.8236
5.2	-8	-0.3505	0.0271	0.8073	1.6532	2.5486	3.5360	3.9812	4.0308	4.8078
5.4	-8	-0.2573	-0.2081	0.0439	0.7513	1.5434	2.1922	2.9820	3.4460	3.8233
5.6	-7	0.1734	0.1758	0.2105	0.7665	1.3160	2.0927	2.6762	3.3937	3.0072
5.8	-7	0.3255	0.0443	0.0350	0.2994	0.7030	1.4115	1.9127	2.4752	2.9270
6.0	-7	-0.0223	-0.0901	-0.0387	0.0066	0.1053	0.7910	1.4902	2.0704	2.6780
6.2	-6	-0.2787	-0.2690	-0.2866	0.3108	0.1913	0.9931	1.5150	2.0422	2.3473
6.4	-6	-0.4189	-0.4214	-0.3855	-0.0788	-0.2093	0.3724	0.8439	1.1771	1.8913
6.6	-5	-0.4534	-0.4509	-0.4457	-0.3908	-0.1809	0.2603	0.6239	1.3040	1.2296
6.8	-5	-0.4624	-0.4618	-0.4610	-0.4526	-0.3944	-0.1513	0.1200	0.6880	1.2531
7.0	-5	-0.4655	-0.4650	-0.4646	-0.4643	-0.4513	-0.3720	-0.1924	0.1764	0.8115
7.2	-4	-0.4701	-0.4699	-0.4692	-0.4655	-0.4420	-0.3443	-0.1038	0.3853	0.5232
7.4	-4	-0.4764	-0.4764	-0.4763	-0.4761	-0.4714	-0.4390	-0.3459	-0.0799	0.2475
7.6	-3	-0.4859	-0.4859	-0.4860	-0.4852	-0.4793	-0.4483	-0.3271	-0.0732	-0.4518
7.8	-3	-0.5001	-0.5001	-0.5001	-0.5001	-0.4995	-0.4930	-0.4522	-0.3304	-0.3680
8.0	-3	-0.5210	-0.5210	-0.5210	-0.5210	-0.5211	-0.5205	-0.5114	-0.4668	-0.4720
8.2	-2	-0.5507	-0.5507	-0.5507	-0.5508	-0.5509	-0.5499	-0.5396	-0.5484	-1.0487
8.4	-2	-0.5911	-0.5911	-0.5911	-0.5911	-0.5913	-0.5919	-0.5925	-0.6302	-0.9487
8.6	-1	-0.6430	-0.6430	-0.6430	-0.6431	-0.6435	-0.6455	-0.6670	-0.8586	-0.7129
8.8	-1	-0.7064	-0.7064	-0.7064	-0.7064	-0.7066	-0.7078	-0.7197	-0.9582	-0.7927
9.0	-1	-0.7805	-0.7805	-0.7805	-0.7805	-0.7805	-0.7811	-0.7872	-0.8944	-0.8244